CrossMark

ORIGINAL

Experimental investigation of impingement heat transfer from a round rib-roughened surface

Mustafa Kemal Isman[1] · Muhiddin Can[2]

Abstract An experimental investigation on impingement heat transfer from a rib-roughened surface is performed. Single, double, and triple rib configurations are tested. The rib is also located at three different positions for a single rib case. The Reynolds number is varied from 10,000 to 50,000 whereas the dimensionless jet-to-surface distance (z/D) is kept constant as 8. Results show that, the Nusselt number decreases just before a rib. After the rib, however, the Nusselt number decreases by a larger amount. Since ribs cause a reincreasing in the Nusselt number after the stagnation point and since the stagnation point Nusselt number is not affected by ribs, they can be used to enhance heat transfer especially for spot cooling applications. It is also obtained that using ribs is more useful for low speed impinging jets, when heat transfer from the whole surface is considered.

List of symbols

D   Jet diameter, m
ε Emissivity of the surface
h   Convective heat transfer coefficient, W/m^2K
k   Thermal conductivity, W/mK
Nu_x Local Nusselt number, $(=hD/k)$
$\dot{q}$ Heat flux, W/m^2
Re   Reynolds number, $(=UD/\nu)$
σ Stefan–Boltzmann constant, $5.67 \times 10^{-8}\ W/m^2K^4$
T   Temperature, K
x   Distance from stagnation point, m
ν Kinematic viscosity, m^2/s
z   Distance between jet and surface, m

1 Introduction

Impinging jets have received considerable attention because of their extremely high heat and mass transfer capability. They are widely used in several heat and mass transfer applications, such as cooling of electronics and turbine blades, drying of papers, fabrics and food products, and glass tempering. Therefore it is not surprising that they have been frequently investigated both numerically and experimentally. In the study of Etemoglu et al. [1], an investigation is carried out to determine the effect of nozzle shape and size on heat transfer under impinging air jets. Experimental results show that the discharged coefficient only varies with velocity and nozzle shapes but not with the nozzle widths or hole diameters. The effects of nozzle diameter on impingement heat transfer and fluid flow are investigated in the study of Lee et al. [2]. The results show that the local Nusselt numbers increase with the increasing nozzle diameter in the stagnation region. An experimental study is performed by Yong et al. [3] to explore heat transfer distributions under staggered or inline array-jets impingement inside a semi-confined channel. An experimental study of an axisymmetric turbulent jet impinging on a semi-cylindrical concave surface is carried out by Hashiehbaf et al. [4]. Their study shows that the position of a secondary peak in the Nusselt number distribution along quasi-flat and curved surfaces is located at y/d = 3.2 and 4.39 < s/d < 5, respectively. In the study of Fenot et al. [5], a multichannel hot jet is investigated experimentally, with and without swirling effects. It is found that the swirling effect mainly affects ambient air entrainment into the jet and consequently effectiveness of heat transfer. The flow characteristics of an isothermal turbulent jet

✉ Mustafa Kemal Isman
   mkisman@gmail.com; mkemal.isman@btu.edu.tr

[1]   Department of Mechanical Engineering, Bursa Technical University, Yildirim Campus, 16330 Bursa, Turkey

[2]   Department of Mechanical Engineering, Uludag University, Gorukle Campus, 16059 Bursa, Turkey

impinging normally on a flat plate is studied experimentally by Yao et al. [6]. It is declared that the normal velocity fluctuations have the greatest skewness and the highest intermittency in the mixing region. Liu et al. [7] investigate the optimal jet-to-surface distance (z/D) for stagnation point heat transfer and the location of the secondary peak in local heat transfer at a small z/D value. The optimal z/D value for the stagnation region Nusselt number is found to be about 5. The location of the secondary peak in the local Nusselt number for z/D of 1.5 is at a radial location (r/D) of about 1.8. Kito et al. [8] perform a study to investigate the enhancement of impingement heat transfer by ribs. The slot jet is used and the rib spacing is focused in their study. It is found that the rib spacing must be more than six times the jet width to improve heat transfer. The impingement heat transfer from rib roughened surface within two-dimensional arrays of circular jet is experimentally investigated by Haiping et al. [9]. It is concluded that the jet hole spacing and the jet-to-surface distance have significant effect on the impingement heat transfer. The micro W shaped ribs are used to enhance the impingement heat transfer by Rao et al. [10]. The experimental and numerical studies are performed to investigate effect of W shaped ribs on the impingement heat transfer. The results show that the micro W ribs can improve the area averaged impingement heat transfer on the test plate by about 9.6 % at Reynolds number of 30,000. Cooling of the rib roughened surface by a row of air jets inside semi-confined channel is experimentally investigated by Tan et al. [11]. Orthogonal, V-shaped, and inverted V-shaped ribs are considered. It is declared that the ribs on the target plate provide stronger convective heat transfer in the wall jet region. A numerical study is performed by Wan et al. [12] to investigate the impingement heat transfer from roughened surface with square pin fins. Numerical results show that the total heat transfer is enhanced by about 60 %, but the heat transfer on the flat portion of the roughened surface is eventually be reduced.

Numerous studies on the impingement heat transfer are performed because of their importance in the industrial applications. In literature, however, there is limited information about effects of ribs on heat transfer, for especially single round jet case. The main objective of the present study is to investigate the effects of ribs attached on the surface on impingement heat transfer. For this aim the ribs are attached on the surface in several configurations and several tests are performed by using unconfined single round jet for three Reynolds numbers.

2 Experimental apparatus and procedure

The experimental setup used in the present study is sketched in Fig. 1. The equipment for the experiments consists of a fan, frequency controller, hose, round jet,

tempered glass as target plate, infra-red (IR) thermometer, air velocity transducer, and data-logger. All experiments are performed in a large enough room kept at a constant temperature. A frequency controlled centrifugal fan is preferred to obtain the desired flow rate for the range of the Reynolds number of interest. A single round jet with a diameter of 25 mm is used in the experiments. To obtain fully developed flow, the entrance length is advised to be $10D_h$ [13]. In the present study, however, a pipe with a length of 20D is used as jet. The fan is connected to the jet with a hose which has a diameter of 50 mm. A wire-mesh deflector is placed at the intersection of the hose and the jet. The dimensionless jet-to-surface distance is described as 8 and this distance is kept constant through the experiments. Air velocity measurements are done by an 8455 thermal anemometer (TSI ™) at the jet exit center. Air velocity transducer has a ceramic sensor with a width of about 1 mm. This sensor is protected by a thin metal frame. The air velocity transducer has been carefully placed at the jet exit to avoid disturbed airflow. After air velocity value is measured and desired value is obtained, the air velocity transducer is removed. Through the experiments, the temperature and humidity of the blown air are measured by an HMP 50 sensor (Campbell Scientific, Inc. ™) placed in the hose.

The velocity value measured at the jet exit center is the maximum value of the velocity. Mean velocity is calculated by using following formula relating mean velocity to maximum velocity [14].

$$U_m = U_{\max}\left(1 + 1.33\sqrt{f}\right)^{-1} \tag{1}$$

where,

$$f = 0.316\,\mathrm{Re}^{-1/4} \tag{2}$$

The similar procedure to obtain mean jet velocity value was applied by Kito et al. [8].

The target plate made of tempered glass is the cap of a vessel with an electrical heater as seen in Fig. 2. When the glass plate is cooled by the impinging air, steam condenses at the bottom side of it. The bottom side of the plate is kept at a constant temperature because of the high heat transfer coefficient of the condensing steam. The temperature is controlled by five T-type thermocouples placed on the bottom surface of the tempered glass. The top side of the glass is painted black for providing a high emissivity surface ($\varepsilon \approx 0.95$). The temperature of the top surface is measured with the IR thermometer (TESTO ™ 845).

The heat flux can be determined with Eq. 3 by using the temperature gradients within the glass plate.

$$\dot{q}(x,y) = \frac{k_{glass}}{\Delta z}\left(T_{top}(x,y) - T_{bottom}\right) \tag{3}$$
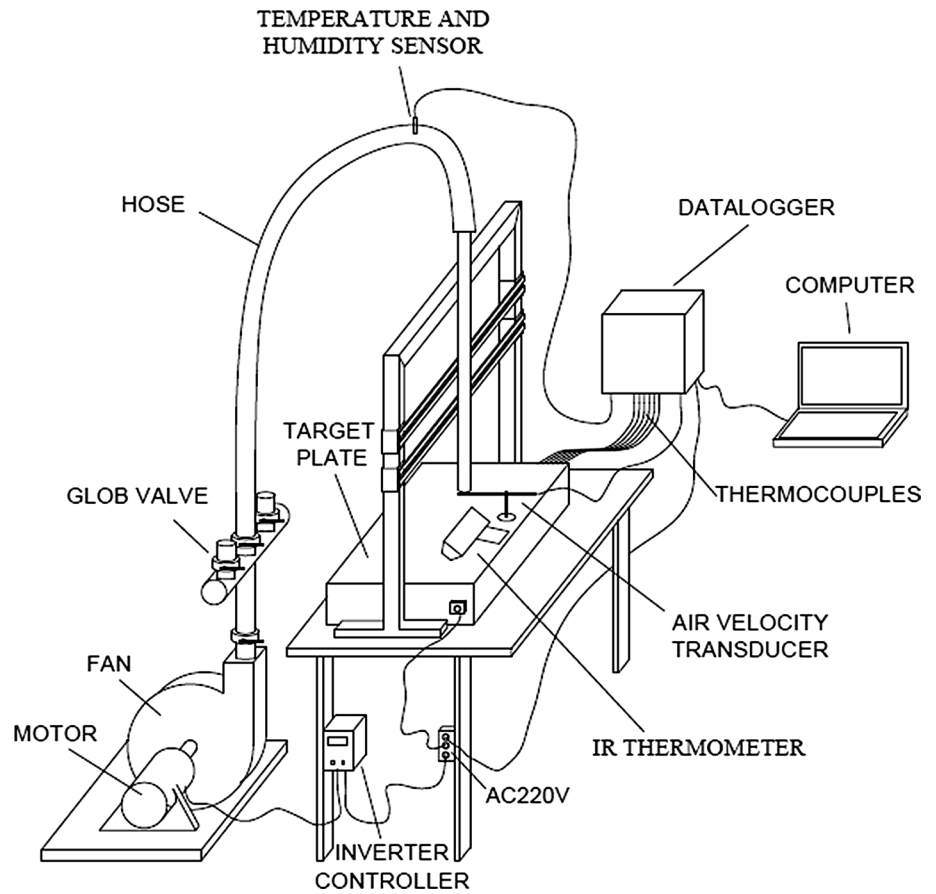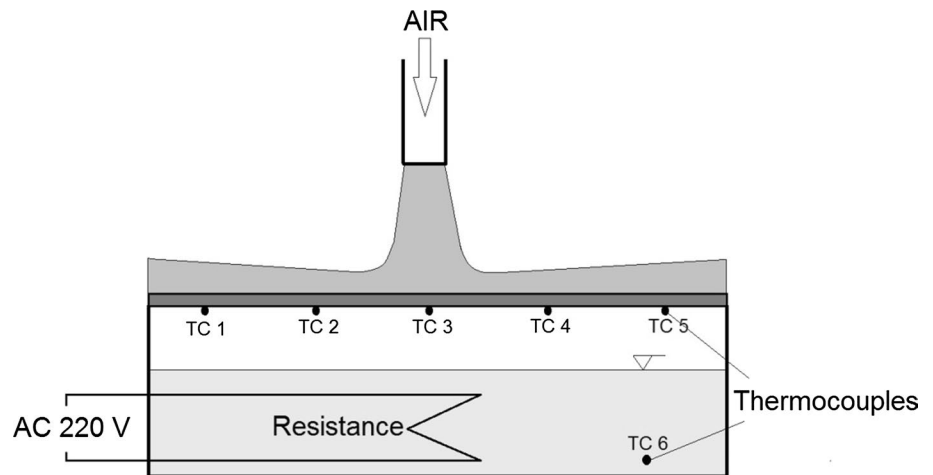
Fig. 1 Experimental set-up

Fig. 2 Detailed experimental chamber

Then local convective heat transfer coefficient (h_x) and local Nusselt number (Nu_x) are calculated as follows:

$$h_x = \frac{\dot{q}(x,y) - \varepsilon\sigma\left(T_{top}^4(x,y) - T_{amb}^4\right)}{\left(T_{top}(x,y) - T_{jet}\right)} \quad (4)$$

$$Nu_x = \frac{h_x D}{k_{air}} \quad (5)$$

This procedure was applied before by Hofmann et al. [15, 16].

The three different Reynolds numbers (Re = 10,000, 30,000, and 50,000) are studied in the present study and they are determined as follows:

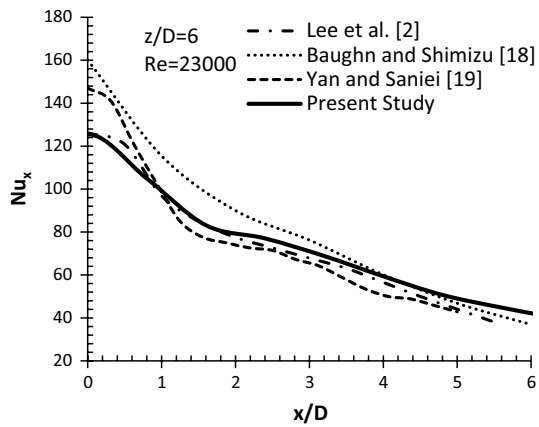$$\text{Re} = \frac{U_m D}{\nu_{air}} \quad (6)$$

Fig. 3 Comparison of the present and previous results

Thermophysical properties of air are evaluated at the jet exit temperature.

The uncertainty analyses for the experimental data are done according to the procedure proposed by Moffat [17]. The uncertainty in the Nusselt and Reynolds numbers is calculated to be less than 6.62 and 6.4 %, respectively.

To validate the results of the present study for a smooth surface, local Nusselt number distribution is compared with that of [2, 18, 19]. As seen Fig. 3, the present results are in good agreement especially with those of [2].

After validation for a smooth surface, ribs are placed on the surface in different configurations as shown in the Fig. 4. These ribs are made of metal with a diameter of 2.5 mm (0.1D) and they are placed on the right and left sides of the jet. Single, double, and triple rib configurations
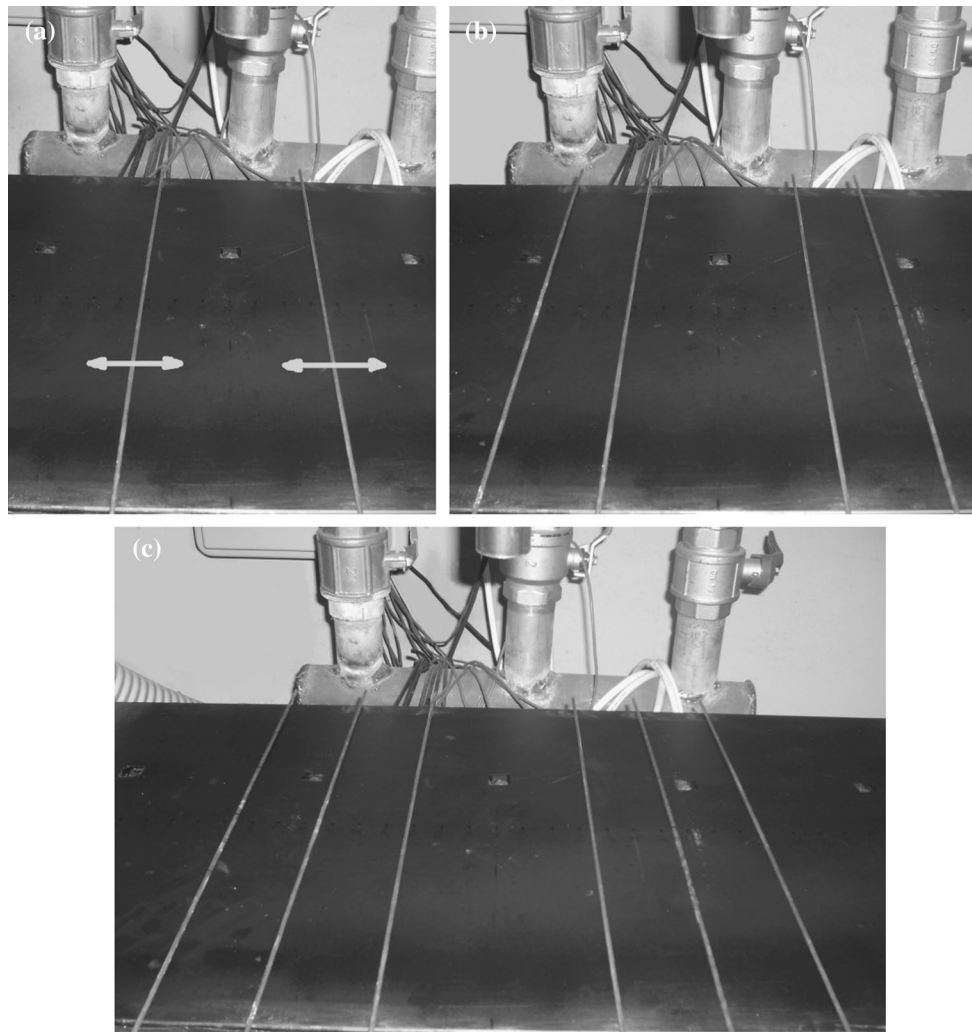

Fig. 4 Different rib cases: **a** single rib, **b** double ribs, and **c** triple ribs

are tested. Three different positions (x/D = 2.5, 5, 7.5) are also examined for a single rib case. The experiments are repeated three times on each configuration and the results are then averaged.

3 Results and discussion

3.1 Effect of ribs on heat transfer

Two single ribs, one for the right and one for the left side of the impinging jet, are placed on the surface. Both ribs are located at 2.5D distance from the impingement point. A comparison of heat transfer from smooth and rib-roughened surfaces is given in Fig. 5 for three different Reynolds numbers.

When the distance between the jet and the surface is larger than that of the potential core, the Nusselt number decreases monotonically with increasing radial distance away from the impingement point. With closer distances, however, a secondary peak in the Nusselt number occurs. According to Gardon and Akfirat [20], a secondary peak in the Nusselt number is the result of a transition from laminar to turbulent boundary layer. It has been also numerically proved by Isman et al. [21]. z/D is especially defined as 8 in the present study so that there is no secondary peak in the Nusselt number for this distance because of laminar to turbulence transition. Thus, the effect of ribs on local Nusselt number distribution can be seen more clearly.

As seen in Fig. 5, the Nusselt number decreases just before the rib for all three Reynolds numbers. The amounts of decrease are 10, 8.2, and 6.7 % for Re = 10,000, 30,000, and 50,000 respectively. Thus, the amount of decrease in the Nusselt number is inversely correlated with the increasing Reynolds number.

The Nusselt number decreases monotonically with increasing radial distance away from the impingement point, since the increasing boundary layer thickness. The air separates from the surface due to the rib and reattaches to the surface after the rib. Thus, the boundary layer is disturbed by the rib and the heat transfer increases. The secondary peak in the Nusselt number occurs behind the rib as seen in Fig. 5. The amounts of increase are 14.8, 16, and 22 % for Re = 10,000, 30,000, and 50,000 respectively. However, unlike at the front of the rib, the amount of increase in the Nusselt number is positively correlated with the increasing Reynolds number. Therefore, when the impingement region (|x/D| ≤ 5) is considered, a single rib case (rib at 2.5D) has more advantages for Re = 50,000 than that of a lower Reynolds numbers, due to a lower decrease and a higher increase in the Nusselt number before and after the rib respectively.
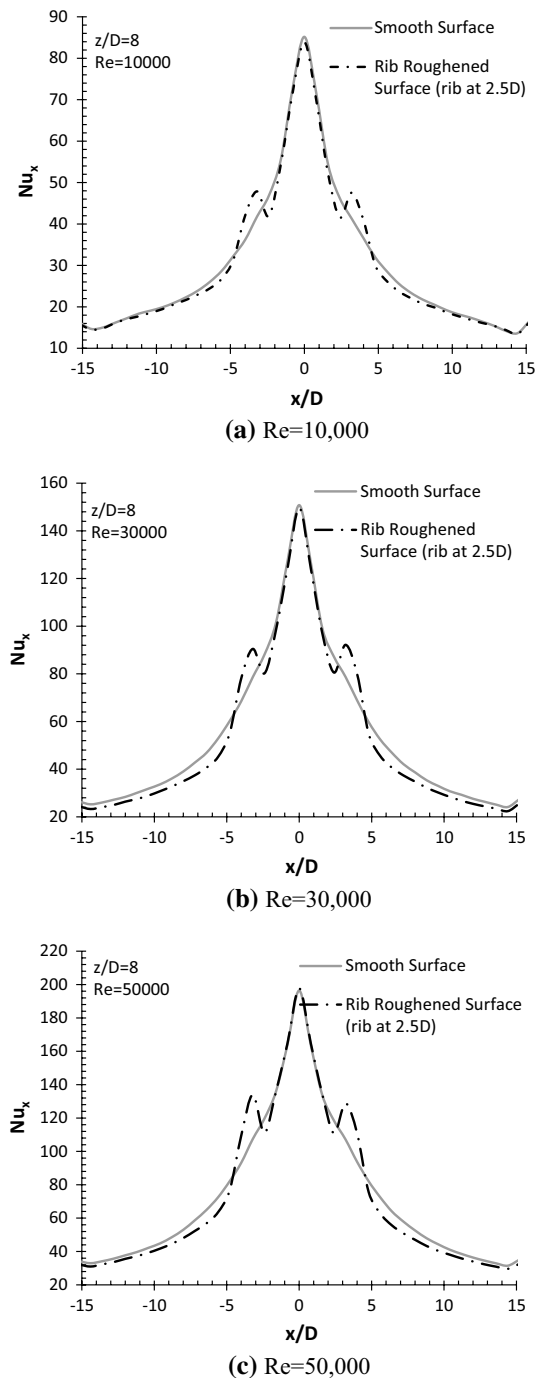

(a) Re=10,000

(b) Re=30,000

(c) Re=50,000

Fig. 5 Comparison of heat transfer from smooth and single rib-roughened (rib at x/D = 2.5) surfaces **a** Re = 10,000, **b** Re = 30,000, and **c** Re = 50,000

As seen in Fig. 5, Nusselt number values recorded in the wall jet region (|x/D| ≥ 5) for the rib-roughened surface is lower than that of a smooth surface case. This difference is low for Re = 10,000, whereas it reaches to 14 % for Re = 30,000. Although this is a disadvantage for

a rib-roughened surface, it is clear that ribs increase heat transfer for |x/D| ≤ 5. Therefore, it can be useful for spot cooling applications such as electronics cooling. Another practical aspect of rib-roughened surfaces is that they do not decrease the Nusselt number for the stagnation point. This result is also obtained by Kito et al. [8] for the stagnation point Nusselt number for L/B ≥ 6.

3.2 Effect of ribs' positions on heat transfer

To investigate the effect of the ribs' position on heat transfer, the ribs are sequentially located at distances of 2.5, 5, and 7.5D from the stagnation point. As seen in Fig. 6, each rib causes a decrease and then an increase in the Nusselt number just before and after the rib. For Re = 10,000, the amounts of decrease in the Nusselt numbers just before the rib are 10, 10, and 6 % for 2.5, 5, and 7.5D rib distances respectively. The amounts of decrease in the Nusselt numbers just before the rib are 8.2, 9.9, and 8 % for Re = 30,000 and 6.7, 7.8, and 8.1 % for Re = 50,000. For Re = 10,000, the amounts of increase in the Nusselt numbers just after rib are 14.8, 12.9, and 8.5 % for 2.5, 5, and 7.5D rib positions respectively. These values are recorded as 16, 21.3, and 23.4 % for Re = 30,000 and 22, 22.4, and 27 % for 50,000. For Re = 30,000 and 50,000, ribs cause a higher increase in the Nusselt number when they are placed farther from the stagnation point. On the contrary, for Re = 10,000, when ribs are placed nearer to the stagnation point, a higher increase in the Nusselt number is seen. For any rib position, the amount of increase in the Nusselt number increases with the increasing Reynolds number. As obtained in the previous section, after the secondary peak, the Nusselt number is recorded as lower for a rib-roughened surface than it is for a smooth surface. The same situation is valid for other rib positions as seen in Fig. 6. However, the difference is very low (max 8 %) for 5 and 7.5D rib positions, even for a high Reynolds number. In fact, there is almost no difference for a rib position of 7.5D for three Reynolds numbers.

3.3 Effect of rib number on heat transfer

Single (2.5, 5, and 7.5D positions), double and triple rib cases are tested and compared in this section. Each test is performed with three Reynolds numbers. As seen in Fig. 7, the increase in the Nusselt number after the rib located at x/D = 2.5D is almost the same for the single (rib at 2.5D), double, and triple rib cases. For the rib located at 5D, however, the maximum increase in the Nusselt number is recorded for a single rib case (rib at 5D). This is because the Nusselt number just before the rib located at x/D = 5 is lower for the double and triple cases than it is for the single rib case, due to the reducing effect of the previous rib
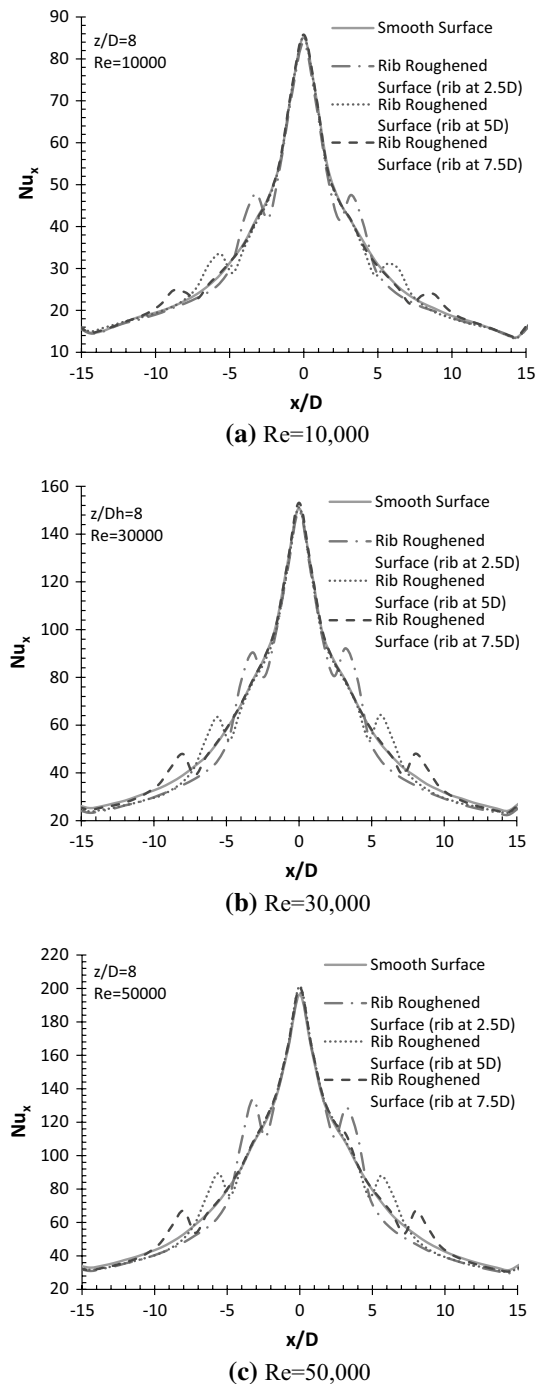

(a) Re=10,000

(b) Re=30,000

(c) Re=50,000

Fig. 6 Effect of the location of a single rib on heat transfer **a** Re = 10,000, **b** Re = 30,000, and **c** Re = 50,000

located at x = 2.5D. On the other hand, there is almost no difference for double and triple cases for this rib position. The maximum increase in the Nusselt number is similarly recorded for the single rib case for the 7.5D rib position, due to the same reason. As seen in Fig. 7, the stagnation point Nusselt number remains almost the same for all configurations.
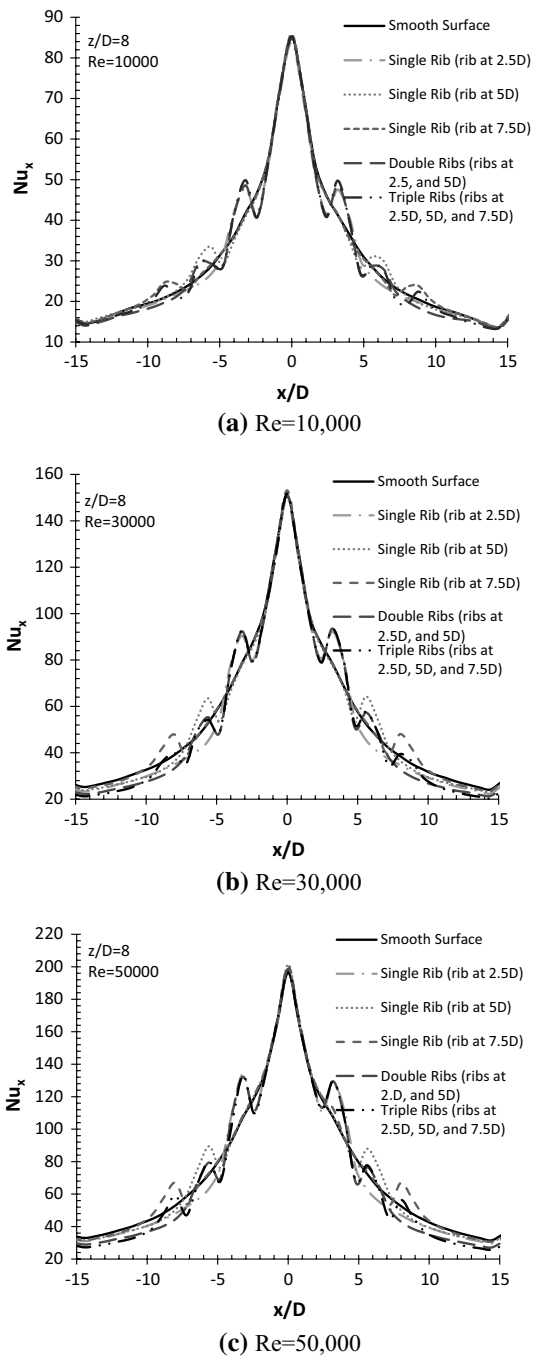
(a) Re=10,000

(b) Re=30,000

(c) Re=50,000

Fig. 7 Effect of number of rib on heat transfer **a** Re = 10,000, **b** Re = 30,000, and **c** Re = 50,000

As mentioned in Sect. 3.1, although heat transfer is increased by the presence of rib, after the secondary peak, the Nusselt number remains lower for the single rib case than it does for the smooth surface case. This difference is low for Re = 10,000, whereas it reaches up to 14 % for Re = 30,000. This was a disadvantage for the single rib case. As seen in Fig. 7, the second and third ribs help to eliminate this disadvantage.

It is clear from Fig. 7.a. that the overall heat transfer for a rib-roughened surface (for almost all rib cases) is higher than that of a smooth surface for Re = 10,000. Therefore, ribs are more useful for low speed impinging jets when the heat transfer from the whole surface is considered.

4 Conclusions

Experimental studies are performed to investigate the effects of ribs on heat transfer with an impinging air jet. Some specific conclusions are summarized as follows.

When a rib is attached on the target surface, the Nusselt number decreases just before the rib, and the secondary peak is shown in the Nusselt number after the rib. The results show that this increase in the Nusselt number is higher than the decrease, independently of the Reynolds number and the rib positions.

The stagnation point Nusselt number is not affected by ribs.

The Nusselt number values recorded in the wall jet region ($|x/D| \geq 5$) for a rib-roughened surface (rib at 2.5D) is lower than that of a smooth surface case. Although this is a disadvantage for rib-roughened surfaces, it is clear that ribs increase heat transfer for $|x/D| \leq 5$. Therefore, ribs can be useful for spot cooling applications such as electronics cooling.

For Re = 10,000, when ribs are placed nearer to the stagnation point, a higher increase in the Nusselt number is seen. On the contrary, for Re = 30,000 and 50,000, ribs cause a higher increase in the Nusselt number when they are placed farther from the stagnation point.

When second or third ribs are attached on the surface, they cause an increase in the Nusselt number. Although the impacts of the second and third ribs are lower than that of a single rib placed at the same location, the second and third ribs help the Nusselt number that is decreased by the first or second rib to increase again.

Results show that overall heat transfer for a rib-roughened surface (for almost all rib cases) is higher than that of a smooth surface for Re = 10,000. Therefore, ribs are more useful for low speed impinging jets, when heat transfer from the whole surface is considered.

References

1. Etemoglu AB, Isman MK, Can M (2010) Investigation into the effect of nozzle shape on the nozzle discharge coefficient and heat and mass transfer characteristics of impinging air jets. Heat Mass Transf 46:1395–1410. doi:10.1007/s00231-010-0666-7
2. Lee DH, Song J, Jo MC (2004) The effects of nozzle diameter on impinging jet heat transfer and fluid flow. J Heat Transf 126:554. doi:10.1115/1.1777583

3. Yong S, Jing-zhou Z, Gong-nan X (2015) Convective heat transfer for multiple rows of impinging air jets with small jet-to-jet spacing in a semi-confined channel. Int J Heat Mass Transf 86:832–842. doi:10.1016/j.ijheatmasstransfer.2015.03.073

4. Hashiehbaf A, Baramade A, Agrawal A, Romano GP (2015) Experimental investigation on an axisymmetric turbulent jet impinging on a concave surface. Int J Heat Fluid Flow 53:167–182. doi:10.1016/j.ijheatfluidflow.2015.03.003

5. Fénot M, Dorignac E, Lalizel G (2015) Heat transfer and flow structure of a multichannel impinging jet. Int J Therm Sci 90:323–338. doi:10.1016/j.ijthermalsci.2014.12.006

6. Yao S, Guo Y, Jiang N, Liu J (2015) An experimental study of a turbulent jet impinging on a flat surface. Int J Heat Mass Transf 83:820–832. doi:10.1016/j.ijheatmasstransfer.2014.12.026

7. Liu Q, Sleiti AK, Kapat JS (2008) Application of pressure and temperature sensitive paints for study of heat transfer to a circular impinging air jet. Int J Therm Sci 47:749–757. doi:10.1016/j.ijthermalsci.2007.06.018

8. Kito M, Takezaki M, Shakouchi T et al (2012) Enhancement of impingement heat transfer on a flat plate with ribs. Int Sch Sci Res Innov 6(8):1623–1629

9. Haiping C, Jingyu Z, Taiping H (1998) Experimental investigation on impingement heat transfer from rib roughened surface within arrays of circular jet: effect of geometric parameters. In: Int. Gas Turbine Aeroengine Congr. Exhib. ASME, Stocholm, Sweden

10. Rao Y, Chen P, Wan C (2016) Experimental and numerical investigation of impingement heat transfer on the surface with micro W-shaped ribs. Int J Heat Mass Transf 93:683–694. doi:10.1016/j.ijheatmasstransfer.2015.10.022

11. Tan L, Zhang JZ, Xu HS (2014) Jet impingement on a rib-roughened wall inside semi-confined channel. Int J Therm Sci 86:210–218. doi:10.1016/j.ijthermalsci.2014.06.037

12. Wan C, Rao Y, Zhang X (2013) Numerical investigation of impingement heat transfer on a flat and square pin-fin roughened plates. In: Proc ASME Turbo Expo 2013 Turbine Tech Conf Expo, San Antonio, Texas, USA

13. Cengel YA (2006) Heat and mass transfer, 3rd edn. McGraw-Hill, Columbus, OH, USA

14. White FM (2015) Fluid mechanics, 8th edn. New York, McGraw-Hill, Columbus, OH, USA

15. Hofmann HM, Kind M, Martin H (2007) Measurements on steady state heat transfer and flow structure and new correlations for heat and mass transfer in submerged impinging jets. Int J Heat Mass Transf 50:3957–3965. doi:10.1016/j.ijheatmasstransfer.2007.01.023

16. Hofmann HM, Movileanu DL, Kind M, Martin H (2007) Influence of a pulsation on heat transfer and flow structure in submerged impinging jets. Int J Heat Mass Transf 50:3638–3648. doi:10.1016/j.ijheatmasstransfer.2007.02.001

17. Moffat RJ (1988) Describing the uncertainties in experimental results. Exp Therm Fluid Sci 1:3–17. doi:10.1016/0894-1777(88)90043-X

18. Baughn JW, Shimizu S (1989) Heat transfer measurements from a surface with uniform heat flux and an impinging jet. J Heat Transf 111:1096–1098. doi:10.1115/1.3250776

19. Yan X, Saniei N (1997) Heat transfer from an obliquely impinging circular, air jet to a flat plate. Int J Heat Fluid Flow 18:591–599. doi:10.1016/S0142-727X(97)00051-9

20. Gardon R, Akfirat JC (1965) The role of turbulence in determining the heat-transfer characteristics of impinging jets. Int J Heat Mass Transf 8:1261–1272. doi:10.1016/0017-9310(65)90054-2

21. Isman MK, Morris PJ, Can M (2016) Investigation of laminar to turbulent transition phenomena effects on impingement heat transfer. Heat Mass Transf 52:2027–2036. doi:10.1007/s00231-015-1719-8